Available online at www.sciencedirect.com
SCIENCE DIRECT®
Cement & Concrete Composites 28 (2006) 212–219
Cement & Concrete Composites
www.elsevier.com/locate/cemconcomp

EIS study of passivation of austenitic and duplex stainless steels reinforcements in simulated pore solutions

G. Blanco [a], A. Bautista [a,*], H. Takenouti [b]

[a] Universidad Carlos III de Madrid, Materials Science and Engineering Department, Avda, Universidad 30, 28911 Leganés, Madrid, Spain
[b] Laboratoires Interfaces et Systèmes Electrochimiques, UPR-15 du CNRS, UPMC, Casier 133, 4 Place Jussieu, 75252 Paris Cedex 05, France

Abstract

Stainless steel reinforcements have proved to be one of the most effective methods to guarantee the passivity of reinforced concrete structures exposed to highly chloride-contaminated atmospheres. In the present work, the corrosion behaviour of two traditional austenitic stainless steels (AISI 304 and 316L types), and one duplex type (2205) are compared with that of a low-nickel, much more economic, austenitic type (204Cu). Ribbed and ground bars of these four materials are studied in non-carbonated and carbonated, saturated $Ca(OH)_2$ solutions with different chloride contents, using electrochemical techniques. The low-frequency time constant represents the charge transfer resistance (R_t) in parallel with the double layer capacitance. The R_t value of the passive reinforcements seems to be related with the quality of the passive layer. R_t values increase with the immersion time in the testing solutions and decrease with the chloride content. Moreover, R_t tends to increase when the ribs of the bars are removed.

Keywords: Stainless steels; Electrochemical impedance spectroscopy (EIS); Passivity; Reinforcements; Simulated pore solutions

1. Introduction

Reinforced concrete is a versatile, economical and successful construction material. It is durable and strong, performing well throughout its service life. Conventional black steel reinforcements embedded in concrete are passive due to a protective, very thin oxide layer (about 10 nm) [1] that is formed on its surface in high alkaline media such as that the contained in the pores of the concrete (pH about 12.6). However, these reinforcements suffer severe corrosion problems when the reinforced concrete structure is exposed to chloride contaminated environments and/or when the concrete cover is carbonated. Chlorides favour localized pitting corrosion of the steel, and carbonation a generalized attack.

Nowadays, cathodic protection and the use of stainless steel reinforcements seem to be the most reliable solutions to guarantee the durability of reinforced concrete structures in extremely aggressive environments [2,3]. Although the use of stainless steel reinforcements can be, at long times, a more economically profitable alternative than cathodic protection [4], the initial cost of using stainless steel has limited their use many times.

Up to now, most of the published literature has focused on the most commercial austenitic stainless steel types, such as AISI 304 and 316, though there are studies about other ribbed stainless steels. The corrosion results obtained for 304 and 316 types have shown the very good behaviour of these materials in chloride-bearing concrete or simulated pore solutions [3–9]. Nowadays, duplex stainless steels are coming into use. Recent works have demonstrated that their corrosion resistance in these media is similar to that of the traditional austenitic types or even better, depending on the composition of the studied duplex steel [5,10,11]. However, ferritic types (the cheapest traditional stainless steels) have demonstrated to be susceptible to pitting corrosion in severe marine environments [12].

* Corresponding author. Tel.: +34 91 624 9914; fax: +34 91 624 9430.
E-mail address: mbautist@ing.uc3m.es (A. Bautista).

0958-9465/$ - see front matter © 2006 Elsevier Ltd. All rights reserved.
doi:10.1016/j.cemconcomp.2006.01.012

Nickel is one of the alloying elements that most raise the cost of such austenitic and duplex stainless steels, above that of other majority alloying elements as chromium. High-manganese, low-nickel austenitic stainless steel has proved to have mechanical properties comparable to those of traditional austenitic steels, and the corrosion resistance in acid and in neutral solutions with chlorides ranges between values very close to that of the type 304 to values intermediate between typical corrosion resistances of austenitic and ferritic types [13]. A recent work has demonstrated that the low-Ni type 204Cu stainless steels have good corrosion behaviour similar to the traditional stainless steels (type 304, 316), in media that simulated concrete pores [14]. The economical advantages that imply the use of this type of reinforcements stress the interest of studying in depth the corrosion behaviour of 204Cu in mortars and simulated concrete pore solutions.

Traditionally, the corrosion resistance of stainless steel reinforcements in simulated concrete pore solutions has been studied through d.c. electrochemical methods, mainly destructive anodic polarizations curves [7,9–11,14]. Some authors have tried to analyse the characteristic of the passive layer formed on stainless steels on alkaline media through electrochemical impedance spectroscopy (EIS) [15,16]. All of them have used equivalent circuit with two time constants to explain the electrochemical response of the stainless steels reinforcements, but the meaning assigned to the equivalent-circuit components depends on the author. Sometimes it is stated that the high-frequency constant inform about the charge transfer process that occurs on the surface of the reinforcements [15] and sometimes the charge transfer process is assigned to the low-frequency constant [16].

The main objective of this work is to explore the possibilities that EIS offers for the study of the quality and the stability of the passive layer formed on the surface of the stainless steel reinforcements in simulated pore solutions of different compositions. For accomplishing this objective, four ribbed stainless steels (type 304, 316L, low-Ni 204Cu and duplex 2205) have been electrochemically characterized during exposure in simulated pore solution.

2. Experimental

Samples of 4 cm length were cut from ribbed bars of stainless steels, two traditional austenitic stainless steels (AISI 304 and 316L types), a low-nickel austenitic (type 204Cu) and one duplex (type 2205). Two stainless steels AISI 316L with different compositions have been studied, one with high content in S (0.0060%) called 316L 1°c and another with low content in S (0.0020%) called 316L 2°c. The chemical composition, the diameter and the forming conditions of the stainless steels are shown in Table 1.

The quality of the passive layer of the materials was studied in $Ca(OH)_2$ saturated solutions by EIS. Fresh, non-carbonated solutions were used to simulate non-carbonated concrete (pH 12.6), and solutions in which the pH had been reduced to about 9 by bubbling CO_2-enriched air were used to simulate carbonated concrete. In both types of solution, different amounts of NaCl were added (in quantities that range from 0% to 5% (w/w)) to test the effect of chloride contamination.

Table 1
Chemical composition of the studied ribbed stainless steels

Tipo AISI	304	316L 1°c	316L 2°c	2205	204Cu
Ribbed	Cold	Cold	Cold	Hot	Cold
ϕ (mm)	8.00	10.00	6.00	12.70	5.00
C	0.0630	0.0210	0.0180	0.0190	0.0600
P	0.0310	0.0400	0.0300	0.0300	0.0180
S	0.0025	**0.0060**	**0.0020**	0.0020	0.0010
Si	0.3120	0.2070	0.3650	0.3160	0.2800
Mn	1.4220	1.6740	1.4410	1.5020	7.9360
Cr	18.3300	17.0470	16.9740	22.4080	16.529
Ni	8.1180	10.2480	11.2090	4.8820	1.9350
Mo	0.2970	2.1710	2.0810	2.7490	0.0680
Ti	0.0040	0.0030	0.0040	0.0060	0.0040
N	0.0447	0.0468	0.0476	0.1439	0.1573
Cu	0.3160	0.3230	0.4970	0.0840	2.6910
Sn	0.0170	0.0090	0.0120	0.0040	0.0110
Co	0.1280	0.1720	0.1310	0.0380	0.0130
B	0.0002	0.0033	0.0052	0.0022	0.0003
Nb	0.0090	0.0050	0.0100	0.0070	0.0050
Al	0.0080	0.0001	0.0001	0.0001	0.0060
V	0.0910	0.0790	0.0870	0.1230	0.1160

EIS measurements were carried out in a potentiostat/galvanostat (Ecochimie, AUTOLAB). The amplitude of sinusoidal voltage perturbation signal was equal to 10 mV rms. Steels were studied in the frequency range from 10^5 to 10^{-3} Hz to observe all phenomena present in materials. The EIS measurements were performed after 2 and 20 h of exposure of the reinforcement to the testing solution. The impedance spectra fitting were carried out with a simplex method. During fitting, the two lowest frequency points of the spectra were sometimes erased because they clearly corresponded to noise caused by the non-stabilities of the system.

The susceptibility to pitting corrosion of the ribbed stainless steels was characterized by cyclic polarization curves in a $Ca(OH)_2$ non-carbonated media with 0.5% NaCl. The measurements were carried out in a potentiostat/galvanostat (PAR, model 263A). The electrochemical measurements were carried out again after 20 h of exposure of the reinforcement to the testing solution. The potential scan rate was 0.17 mV/s. The current limit for reversing the sign of the potential sweep was 10^{-4} A/cm^2.

The employed electrochemical cell, both for EIS and polarization curves, was a standard three-electrode system. Working electrodes were made of investigated stainless steels in which its cross sections were ground with SiC paper of decreasing grit size from 180 to 320. Two centimeter of ribbed bars with ground cross sections were introduced into the solution to be analyzed. Saturated calomel electrode (SCE) and graphite bars were used respectively as reference electrode and counter-electrodes.

To study the effect of the corrugations on the electrochemical behaviour of the stainless steels, some ribbed bars have been machined in the shape of cylinders of 4 mm of diameter in order to remove the rib. The surfaces of the cylinders have been ground with SiC paper of decreasing grit size from 180 to 320 before the EIS spectra of these materials have been obtained in non-carbonated, saturated $Ca(OH)_2$ solutions with 1% NaCl, following the same procedure described for ribbed bars.

A detail scanning electron microscopy (SEM) study was carried out to detect the presence of small precipitates in the 316L AISI type stainless steels. The composition of the precipitates has been determined by semiquantitative X-ray dispersive spectroscopy (XDS).

Finally, mechanical tests have been carried out in some specimens to obtain more information about properties as grain size or deformation of the microstructures that can also influence the corrosion behaviour. Tensile tests have been carried out following the EN10002-1 standard. Ultimate tensile strength (UTS) and yield strength (σ_y) have been measured. Vickers hardness (HV30) has been measured in the core the ribbed bars, and microhardness measurements (HV100g) have been carried out in the ribs as well as in the cores.

3. Results and discussion

The anodic cyclic polarization curves (Fig. 1) show that, in non-carbonated, chloride-contaminated media, 2205 duplex stainless steels are not susceptible to pit by imposing anodic overpotentials, because O_2 evolution occurs before their pitting potential (E_{pit}) can be reached. All the studied austenitic stainless steels pit at potentials sufficiently high to ensure their passivity in usual working conditions. The 204Cu type exhibits in this medium a corrosion resistance very similar to 304 type, whose immunity to corrosion in concrete structures exposed in aggressive environments have been proved for decades [2]. However, the E_{pit} value of the steel type 316L 1°c (about 550 mV) is significantly minor than that of 316L 2°c (about 700 mV). The main difference between these two 316L stainless steels is their S content (Table 1). After a careful SEM study very small MnS precipitates of 3 μm of length were found in the 316L 1°c. Fig. 2 shows the precipitates found in this stainless steel. Though the S content in 316L 1°c is not especially high the presence of this precipitates has previously been detected in other 316 stainless steels with similar Cr and Mn content [17]. The influence of MnS inclusions in the pitting of stainless steels is well known, because it has been demonstrated that their partial dissolution allow them to act as preferred sites for pit initiation [18,19]. No precipitate has been found in 316L 2°c bars. Other differences as grain size or grain shape of the austenite are difficult to evaluate objectively using only microscopical observation.

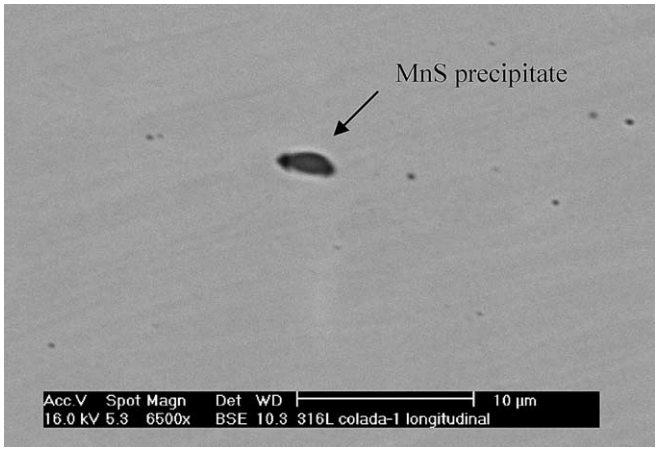

Fig. 2. MnS precipitate present in the stainless steel 316L 1°c.

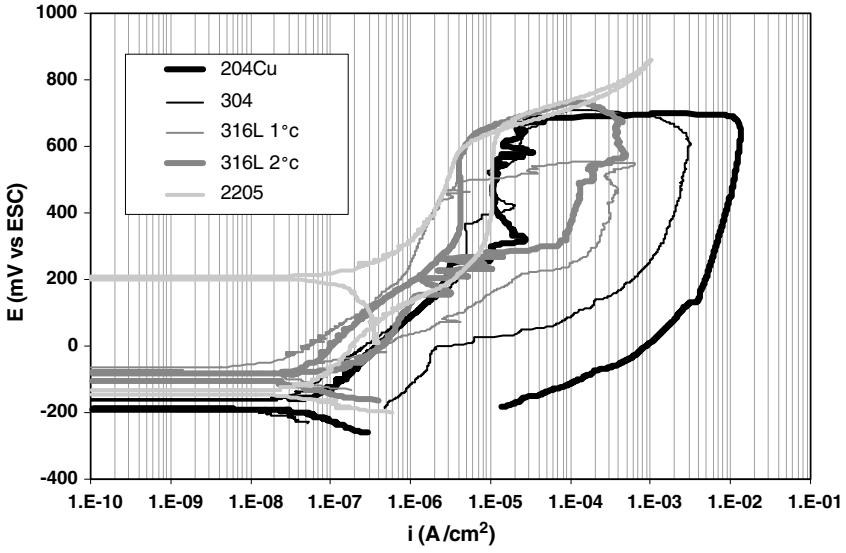

Fig. 1. Polarization curves obtained with different alloy specimen in non-carbonated, saturated $Ca(OH)_2$ solutions with 0.5% NaCl.

Table 2
Mechanical properties of the studied 316L AISI types

Ribbed stainless steels	Tensile test		HV 30	HV 100g	
	UTS (MPa)	σ_y (MPa)	Core	Rib	Core
316L 1°c	805	651	250	329	227
316L 2°c	897	710	270	423	242

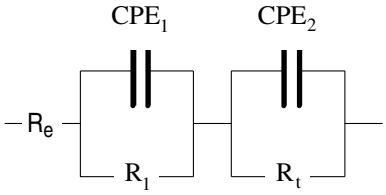

Fig. 3. Equivalent circuit proposed to fit the experimental EIS data.

However, mechanical results as those summarized in Table 2 show that the 316 1°c has the lowest UTS, σ_y, HV30 and HV100g in the core and in the rib of the bars. The higher mechanical properties of the 316 2°c can be caused only by a higher deformation or a lower grain size, and both factors tend to decrease the corrosion resistance. As the surface roughness of both materials is apparently very similar, only the precipitates could be blamed on the worse corrosion behaviour of 316 1°c.

Numerous EIS measurements have been performed to characterize the corrosion behaviour of the studied ribbed steels in $Ca(OH)_2$ solution with different pH and chloride contents. The equivalent circuit proposed to fit the obtained experimental EIS data is shown in Fig. 3. Both capacitors in the figure have been simulated as constant phase elements (CPE). The equivalent circuit with two time constants in parallel, that other authors use for studies carried out in similar (but not identical) conditions [15], gives slightly higher errors in our case. This circuit has also been used to simulate the electrochemical behaviour of passive

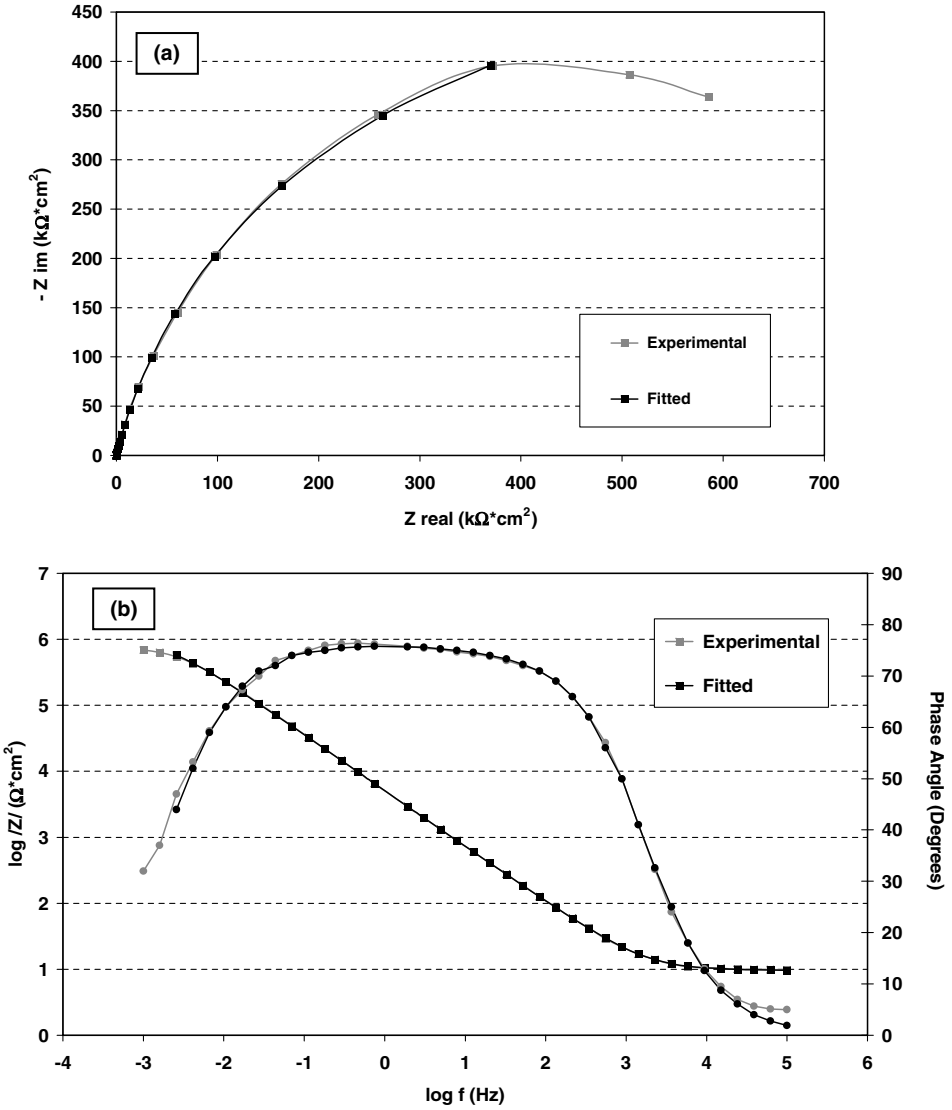

Fig. 4. Impedance spectra for AISI 316L 1°c in $Ca(OH)_2$ with 5% NaCl experimental and fitted data: (a) Nyquist diagram and (b) Bode diagram.

metals that do not suffer corrosion, as stainless steels [20] or titanium [21] in non-aggressive media. Anyway, the values obtained for low-frequency resistance (in which are based most of the paper discussion) with parallel and series circuits for the same spectra are very similar and only meaningful differences can be detected on CPE values. An example of the shape of the spectra and quality of the fitting achieved using equivalent circuit in Fig. 3 is shown in Fig. 4. As it can be observed, the two time constants are significantly overlapped.

The meaning suggested for the circuit components is the following: the low-frequency time constant represents the charge transfer process, and its composed by the charge transfer resistance (R_t) in parallel with the double layer capacitance (CPE_2); the medium-frequency time constant (R_1 and CPE_1) seems to be related with a redox reaction on the material surface; the resistance that appears at very high frequencies corresponds to the ohmic resistance of the solution (R_e). It has been considered the low-frequency constant time as the constant responsible the charge transfer because of the values of R_t (substituting in the Stern–Geary equation) corresponds with corrosion intensities (i_{corr}) similar to those obtained from d.c. measurements [14]. The values determined for R_1 oscillate a lot, probably because the difficulties of analyze spectra with so overlapped time constants. Anyway, for all the materials and solutions tested, R_1 are always meaningfully lower than R_t.

The results of parameter regression with the equivalent circuit presented in Fig. 3 are illustrated in Fig. 4. The capacity of CPE_2 ranges from 50 to 150 $\mu F/cm^2$, typical of a double layer capacitor, as can be seen in Fig. 5. This observation corroborates the assignment of the low-frequency time constant to the charge transfer process. The high-values of R_t obtained for stainless steels in alkaline media make that the time constant corresponding to the charge transfer step appears at frequencies lower than usual.

It can also be observed in Fig. 5 that CPE_1 values are always higher than CPE_2. The order of magnitude of CPE_1 capacitors is compatible with capacitors of a redox process as that which occurs on the outer region of the passive layer. This region is rich in Fe oxides [22] and the redox reaction that can occur at the corrosion potential that exhibit the stainless steels in those media (besides the corrosion process) is the transformation of γ-FeOOH to magnetite, as has been studied in depth by other authors [15,23–25]. Its influence of this phenomenon on the EIS spectra has also been suggested previously [15,25]. The values obtained for R_1 from the EIS spectra are about three orders of magnitude lower than those obtained for R_t.

It is noteworthy that the CPE_2 values are meaningfully higher for duplex stainless steel (2205) than other austenitic stainless steels in all cases examined. The values of the α coefficient corresponding to the CPE_2 vary between 0.7 and 1.0. Minor values have been found for α coefficient corresponding to the CPE_1 usually ranging between 0.5 and 0.7. Low values for α have also been detected by other authors in carbon steel in concrete, due to the presence of heterogeneities of concrete-rebar interface [26,27].

The effect of chloride content of synthetic concrete pore solutions to the R_t values showed that R_t decreases when the chloride content increases (Fig. 6). These results prove the ability of this parameter, obtained from EIS measurements, to characterize the aggressiveness of the media at which the reinforcement is exposed. It is obvious that the presence of chlorides does not only decrease E_{pit} in polarization curves [14], but also affects the protective property of the passive layer in the non-polarized state.

It has also been observed that R_t is always higher in carbonated than in non-carbonated media for all the materials (Fig. 6). This fact is at first sight surprising, because carbonated media is believed to be more aggressive for the reinforcements that non-carbonated media. However, the i_{corr} determined in the non-polarized state using d.c. measurements is also lower in carbonated than in non-carbonated solutions [14,28]. Fig. 7 shows the good correspondence existing between the i_{corr} obtained for the studied materials with a.c. and d.c. electrochemical techniques. i_{corr} values have been calculated from polarization curves and using R_t from EIS spectra. In this last case R_t has been identified with the polarization resistance of the materials and the Stern–Geary expression [29] has been used. The

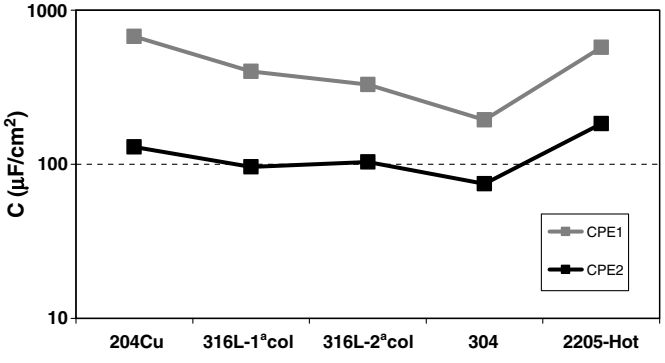

Fig. 5. Values of the capacitors for the stainless steels studied in a non-carbonated $Ca(OH)_2$ solution with 1% NaCl after 18 h of exposure time.

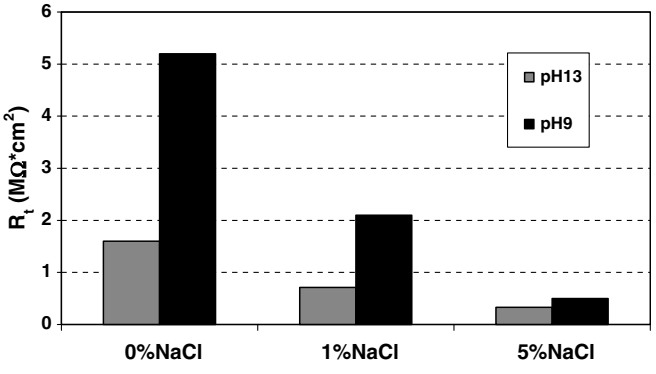

Fig. 6. Influence of the pH and the chloride content media in the value of R_t for the 204Cu stainless steel after 18 h of exposure in the test solution.

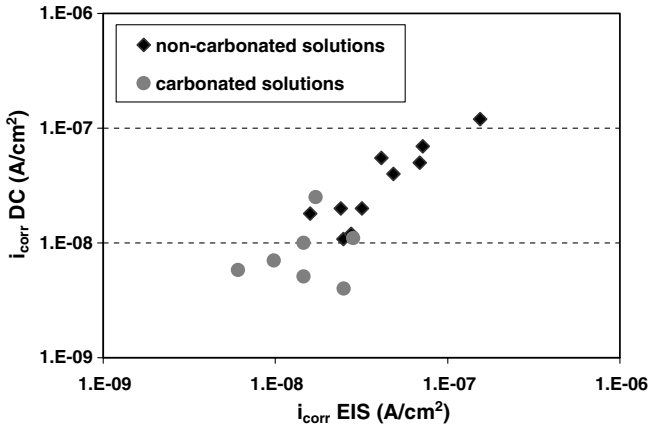

Fig. 7. Relation between values of i_{corr} obtained from direct current (d.c.) measurements and EIS measurements for all the media and materials studied.

measurements performed with the first technique have errors that range between 2% and 3% and for those performed with the second, the errors vary between 8% and 11%. Anyway, though the i_{corr} of the stainless steels reinforcements are always higher at pH 12.6 than at pH 9 at the non-polarized state, the reinforcements need minor overpotentials to achieve meaningful values for the intensities in carbonated solutions than in non-carbonated solutions [7,21].

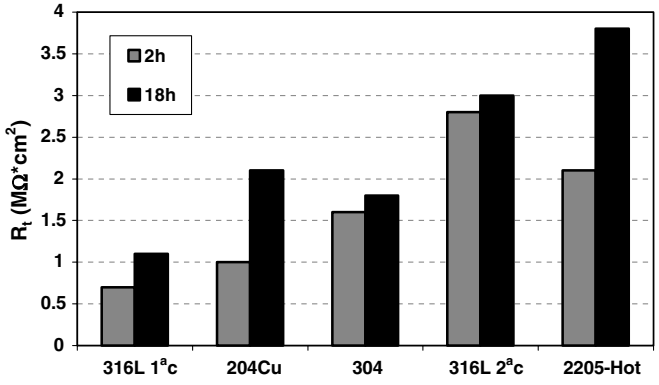

Fig. 8. Influence of the exposure time on the value of R_t for all the materials in carbonated, saturated $Ca(OH)_2$ solution with 1% NaCl.

The value of R_t always increases with the exposure time in the test solution (Fig. 8). This increase in the R_t value reflects the increases of the protective ability of the passive layer that occurs when the stainless steels reinforcements are exposed in alkaline solutions [10,11]. Some relation between the length of the passive zone of the polarization curves for different stainless steels [14] and the R_t value can be guessed from data corresponding to carbonated, saturated $Ca(OH)_2$ solution with 1% NaCl. However, this trend is not so clearly observed in all the media tested. Maybe, the relatively small differences that could exist among the R_t values of the reinforcement, depending on the composition of the stainless steels, are masked by the uncertainties of regression calculation (that are unavoidable when the two time constants of the spectra are as close as in this case).

The ribs have suffered the stronger mechanical deformation in the rebar (compare microhardness values corresponding to the rib and the core in Table 2). The microstructure shows lower grain size in the cross section and more lines corresponding with deformation planes (Fig. 9) in ribs than in remaining metal. For this reason, pits tend to nucleate in the ribs when high anodic

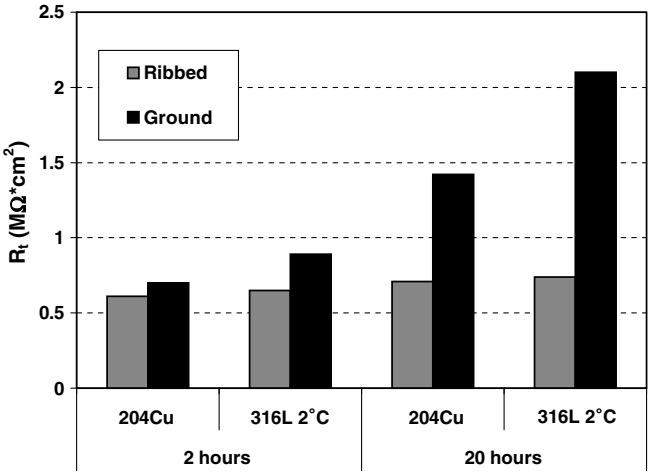

Fig. 10. Influence of the mechanical deformation and geometrical heterogeneities of material surfaces on the R_t values for different exposure times in non-carbonated solution with 1% NaCl.

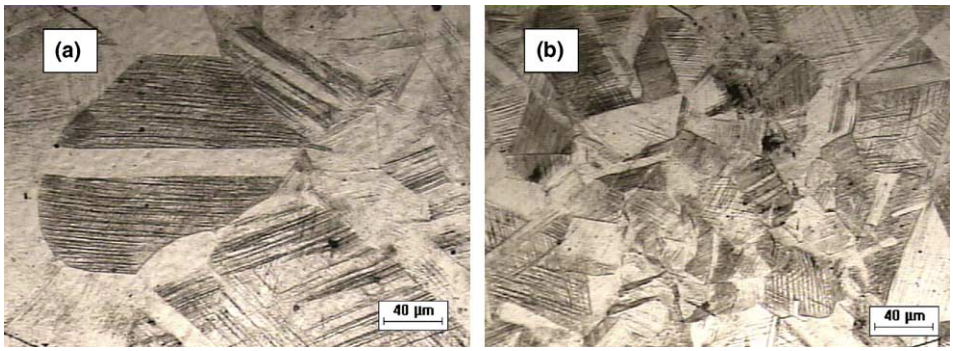

Fig. 9. Microstructure of a cross sectional view of the AISI 304 austenitic stainless steel (a) in the remaining metal and (b) in the rib.

overpotentials are imposed to the stainless steels reinforcements [28]. After removing the outer region of the ribbed bars, the impedance spectra of the materials show higher values of R_t, as can be seen in Fig. 10. After 2 h of exposure in the testing solution, the differences are small, but they tend to increase with time. The quality of the passive layer formed in the materials with a more homogeneous surface and a less deformed microstructure is higher than the quality of the layer formed on stainless steels with ribs.

4. Conclusions

The most important conclusions that can be drawn from the results presented in this work are:

- The equivalent circuit proposed to fit the corrosion behaviour of stainless steels in media that simulated concrete pores is the circuit composed of two time constants besides the ohmic resistance of the solution. The low-frequency time constant represents the charge transfer resistance in parallel with the double layer capacitance and the medium-frequency is related a redox reaction on the material surfaces.
- The value of the charge transfer resistance obtained from EIS measurements increases with the time and decreases with the chloride content, so the technique can inform about changes of protective ability of the passive layers depending on the composition of the media and the exposure time.
- The influence of the composition of the ribbed bars on the charge transfer resistance measured at their non-polarized state is very small and this technique is not useful to predict the differences on their pitting susceptibility.

Acknowledgements

The authors thank the company Roldán S.A. (ACERINOX group) of Spain for providing the ribbed stainless steels used in this study, and the Spanish Ministry of Science and Technology for the financial support provided through the project MAT2004-06435-C02-02. The authors also wish to thank EFC to allow us the publication of this work.

References

[1] Gancedo JR, Alonso C, Andrade C, Gracia M. AES study of the passive layer formed on iron in saturated $Ca(OH)_2$ solutions. Corrosion 1989;45(12):976–7.
[2] Castro-Borges P, de Rincón OT, Moreno EI, Torres-Acosta AA, Martínez-Madrid M, Knudsen A. Performance of a 60-year old concrete pier with stainless steel reinforcement. Mater Perform 2002;41(10):50–5.
[3] Knudsen A, Jensen FM, Klinghoffer O, Skovsgaard T. Cost-effective enhancement of durability of concrete structures by intelligent use of stainless steel reinforcement, Conference on corrosion and rehabilitation of reinforced concrete structures, Florida, USA; 1998.
[4] Kinghoffer O, Frolund T, Kofoed B, Knudsen A, Jensen FM, Skovsgaard T. Practical and economical aspects of application of austenitic stainless steel, AISI 316, as reinforcement in concrete. In: Mietz J, Polder R, Elsener B, editors. Corrosion of reinforcement in concrete. London: IOM Communications; 2000. p. 121–33.
[5] Nürnberger U (editor). Stainless steel in concrete. State of the art report, Publication no. 18, Institute of Materials, London, UK; 1996.
[6] Hewitt J, Tullmin M. Corrosion and stress corrosion cracking performance of stainless steel and other reinforcing bar materials in concrete. In: Swamy RN, editor. Corrosion and corrosion protection of steel in concrete. Sheffield Academic Press; 1994. p. 527–39.
[7] Escudero ML, García-Alonso MC, Capilla F, González JA. Study of the corrosion resistance of stainless steel in solution simulating concrete. In: 15th international corrosion congress, Granada, Spain; 2002.
[8] Sorensen B, Jensen PB, Maanhn E. The corrosion properties of stainless steel reinforcement. In: Page CL, Treadaway CKJ, Bamforth PB, editors. Corrosion of reinforcement in concrete. Elsevier Applied Science; 1990. p. 601–10.
[9] Castro H, Rodríguez H, Belzunce FJ. Mechanical behaviour and corrosion resistance of stainless steel cold rolled reinforcing bars. Mater Sci Forum 2003;426-432:1541–6.
[10] Bertolini L, Bolzoni F, Pastore T, Pedeferri P. Behaviour of stainless steel in simulated concrete pore solution. Br Corros J 1996;31(3):218–22.
[11] Bertolini L, Pedeferri P. Laboratory and field experience on the use of stainless steel to improve durability of reinforced concrete. Corros Rev 2002;20(1/2):129–52.
[12] Callaghan BG. The performance of a 12% chromium steel in concrete in severe marine environments. Corrosion Science 1993;35(5–8): 1535–41.
[13] Raja S, Ramkumar A. Comparative study of intergranular corrosion behaviour of three high manganese austenitic stainless steels. Br Corros J 1996;31(2):153–7.
[14] Bautista A, Blanco G, Velasco F. Resistencia a la corrosión en disoluciones de $Ca(OH)_2$ con cloruros de armaduras de aceros inoxidables austeníticos y dúplex. VIII Congreso Nacional de Materiales, Valencia, Spain; 2004.
[15] Abreu CM, Cristóbal MJ, Losada R, Nóvoa XR, Pena G, Pérez MC. High frequency impedance spectroscopy study of passive films formed on AISI 316 stainless steel in alkaline medium. J Electroanal Chem 2004;572:335–45.
[16] Gu P, Elliot S, Beaudoin JJ, Arsenault B. Corrosion resistance of stainless steel in chloride contaminated concrete. Cem Concr Res 1996;26(8):1151–6.
[17] Noh JS, Laycock NJ, Gao W, Wells DB. Effects of nitric acid passivation on the pitting resistance of 316 stainless steel. Corros Sci 2000;42:2069–84.
[18] Suter T, Webb EG, Böhni H, Alkire RC. Pit initiation on stainless steels in 1 M NaCl and without mechanical stress. J Electrochem Soc 2001;148(5):B174–85.
[19] Schuki P, Hildebrand H, Friedrich A, Virtanen S. The composition of the boundary region of MnS inclusions in stainless steel and its relevance in triggering pitting corrosion. Corros Sci 2005;47: 1239–50.
[20] Rondelli G, Torricelli P, Fini M, Giardino R. In vitro corrosion study by EIS of nickel-free steel for orthopaedic applications. Biomaterials 2005;26:739–44.
[21] Pan J, Leygraf C, Thierry D, Ektessabi AM. Corrosion resistance for biomaterial applications of TiO_2 film deposited on titanium and stainless steel by ion-beam-assisted sputtering. J Biom Mater Res 1997;35:309–18.
[22] Abreu CM, Cristóbal MJ, Nóvoa XR, Pena G, Pérez MC, Rodíguez RJ. Modifications of the stainless steels passive films induced by cerium implantation. Surf Coat Technol 2002;158–159:582–7.

[23] Abreu CM, Cristóbal MJ, Montemor MF, Nóvoa XR, Pena G, Pérez MC. Galvanic coupling between carbon steel and austenitic stainless steel in alkaline media. Electrochem Acta 2001;47: 2271–9.
[24] Veleva L, Alpuche-Aviles MA, Graves-Brook MK, Wipf DO. Comparative cyclic voltammetry and surface analysis of passive films grown on stainless steel 316 in concrete pore model solutions. J Eletroanal Chem 2002;537:85–93.
[25] Abreu CM, Cristóbal MJ, Losada R, Nóvoa XR, Pena G, Pérez MC. Comparative study of passive films of different stainless steels developed on alkaline medium. Electrochem Acta 2004;49: 3049–56.
[26] Sagües AA, Krant SC, Moreno EI. The time domain response of a corroding system with constant phase angle interfacial component: application to steel in concrete. Corros Sci 1995;37(7):1097–113.
[27] Feliu V, González JA, Andrade C, Feliu S. Equivalent circuit for modelling the steel-concrete interface1. Experimental evidents and theoretical predictions. Corros Sci 1998;40(6):975–93.
[28] Bautista A, Blanco G, Velasco F. Corrosion behaviour of low-nickel austenitic stainless steels reinforcements: a comparative study in simulated pore solutions. Cement Concr Res, in press.
[29] Stearn M, Geary A. Electrochemical polarization. I. A theoretical analysis of the shape of polarization curves. J Electrochem Soc 1957;104(1):56–63.